

Supporting Information

Experimental oxygen vacancy formation energies

The temperature-independent oxidation reaction enthalpies correspond to the negative of the oxygen vacancy formation energies $-E_V$; in other words, the LB oxidation reactions are given by $\frac{1}{2}O_{2(g)} + V_O^{\cdot\cdot} + 2B_B^x \rightarrow O_O^x + 2B_B'$ and are reported in the main article for LB and LSB64 compositions with $\delta=0.01$ and $\delta=0.1$, respectively. For a consistent comparison, the effects of charge disproportionation (e.g. $2B^{3+} = B^{4+} + B^{2+}$) are excluded from the experimental reaction enthalpies because these effects are not accounted for in our calculations at 0 K.

Extrapolated and interpolated experimental values

The LSCr64 experimental E_V and $\Delta H_{f,oxide}$ that we report have been extrapolated from measured values for $La_{1-x}Sr_xCrO_3$ with $x=0.1, 0.2, \text{ and } 0.3$.^{1,2} The LSM64 experimental $\Delta H_{f,oxide}$ has been interpolated from measured values for $La_{1-x}Sr_xMnO_3$ with $x=0.1, 0.3, \text{ and } 0.5$.

Additional results

Figure S1 shows effective Bader charges on TM B and O ions in stoichiometric LB and LSB64 compositions. Significant differences between the effective charges on TM B and O ions and their formal oxidation states indicate the covalent nature of the B-O bonding. In addition, the nonlinear trend in the degree of covalency of the TM B-O bonds, which is indicated by the magnitude of the charge difference from the formal oxidation states, suggests that B-O bond covalency alone cannot account for the linear trends in the oxide enthalpies of formation $\Delta H_{f,oxide}$ as a function of the atomic number of B.

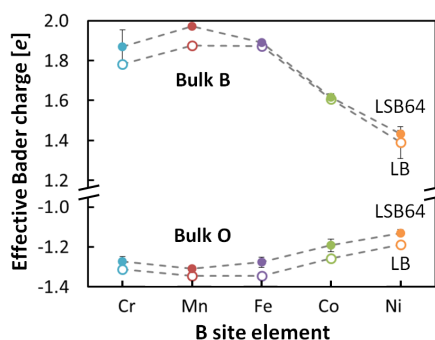


Figure S1 Average effective Bader charges on TM B and O ions in stoichiometric LB and LSB64 compositions. La and Sr effective Bader charges are independent of composition with average values of 2.16 ± 0.01 and 1.59 ± 0.01 e, respectively.

Figure S2 shows the total densities of states (TDOS) for the stoichiometric and oxygen deficient LB and LSB compositions. Redistribution of the excess electron density due to oxygen vacancy V_O formation fills previously unoccupied states; consequently, a higher energy state becomes the highest occupied state and the corresponding energy of the highest occupied state E_{HOS}

increases. The magnitude of the increase in E_{HOS} roughly trends with the magnitude of the energy difference between the lowest unoccupied state and the highest occupied state ΔE . As a result, the insulating LB compositions which exhibit large ΔE also exhibit large increases in E_{HOS} upon V_O formation which in turn contributes to high E_V . In contrast, the LSB64 compositions exhibit negligible ΔE due to the low energy unoccupied states created as a result of the Sr-substitution. These negligible ΔE significantly decrease E_V due to the corresponding small E_{HOS} increases.

As with cation configurations, different V_O configurations gave small variations in the oxygen deficient LSB64 DOS, but characteristic features remained consistent. The energy scale has been aligned so as to match the O 2s core states. These results are consistent with previous calculations of $Ba_{0.5}Sr_{0.5}Co_{1-y}Fe_yO_3$ where the PDOS directly above E_{HOS} is higher for Co than for Fe resulting in lowered E_V with increasing fraction of Co.

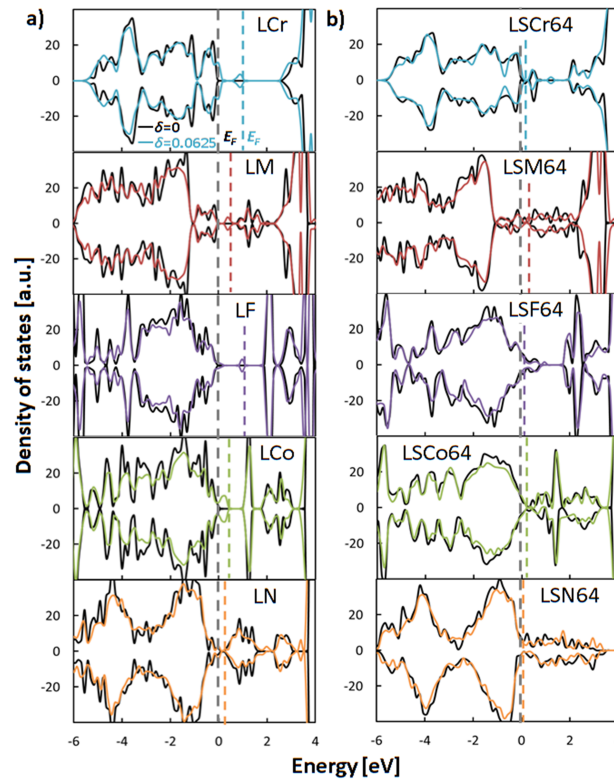


Figure S2 Total densities of states for 80 atom stoichiometric (black, $\delta = 0$) and oxygen deficient (colored, $\delta = 0.0625$) a) LB and b) LSB64 compositions. The energy scale is adjusted to align the O 2s states, and the corresponding energies of the highest occupied states are indicated by dashed lines. Spin-up and spin-down DOS are shown as positive and negative values, respectively.

Figure S3 illustrates the correlation between E_V and the individual parameters $\Delta H_{f,oxide}$ and ΔE . The improved correlation of the combined $\Delta H_{f,oxide}$ and ΔE descriptor with E_V as

compared to either of the individual parameters alone is reflected by increasing R^2 values of 0.67, 0.72, and 0.94 for linear regression fits for only $\Delta H_{f,oxide}$, only ΔE , and for the combined parameter, respectively.

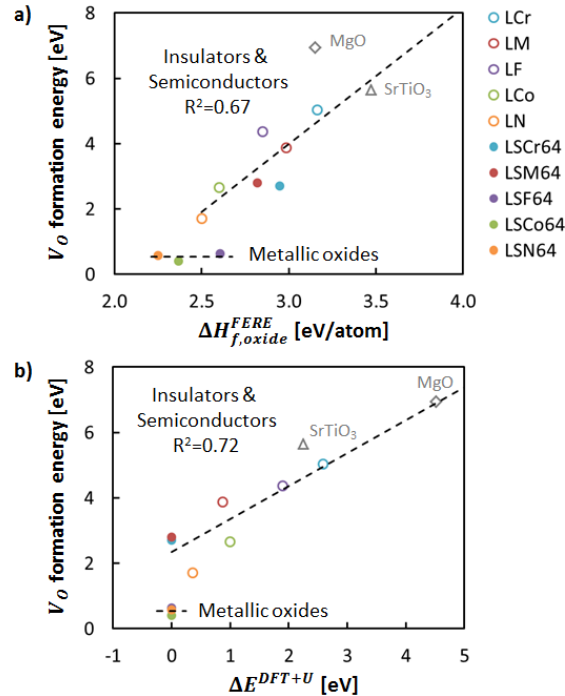


Figure S3 Oxygen vacancy formation energies for LB and LSB64 compositions as a function of a) calculated oxide enthalpies of formation $\Delta H_{f,oxide}$ and b) calculated band gap energies calculated as the difference between the energies of the lowest unoccupied state and the highest occupied state ΔE . Only nonmetallic LB and LSB64 compositions were used in the fits, although the lines are extended for comparison with MgO and SrTiO₃. The corresponding R^2 values are provided for comparison with the $R^2=0.94$ for E_V as a function of the combined $\Delta H_{f,oxide}$ and ΔE parameter.

References

1. J. Mizusaki, S. Yamauchi, K. Fueki, and A. Ishikawa, *Solid State Ionics*, 1984, **12**, 119–124.
2. J. Cheng and A. Navrotsky, *J. Solid State Chem.*, 2005, **178**, 234–244.
3. E. A. Kotomin, Y. A. Mastrikov, M. M. Kukulja, R. Merkle, A. Roytburd, and J. Maier, *Solid State Ionics*, 2011, **188**, 1–5.